Biomedicine & Pharmacotherapy 126 (2020) 110062

Contents lists available at ScienceDirect

Biomedicine & Pharmacotherapy

journal homepage: www.elsevier.com/locate/biopha

IMMUNEPOTENT CRP plus doxorubicin/cyclophosphamide chemotherapy remodel the tumor microenvironment in an air pouch triple-negative breast cancer murine model

Silvia Elena Santana-Krímskaya[a], Moisés Armides Franco-Molina[a,*], Diana Ginette Zárate-Triviño[a], Heriberto Prado-García[b], Pablo Zapata-Benavides[a], Felipe Torres-del-Muro[a], Cristina Rodríguez-Padilla[a]

[a] Universidad Autónoma de Nuevo León (UANL), Facultad de Ciencias Biológicas, Laboratorio de Inmunología y Virología, P.O. Box 46 "F", 66455, San Nicolás de los Garza, NL, Mexico

[b] Instituto Nacional de Enfermedades Respiratorias, Departamento de Enfermedades Crónico-Degenerativas, Tlalpan 4502, Colonia Sección XVI, 14080, Ciudad de México, DF, Mexico

ARTICLE INFO

Keywords:
IMMUNEPOTENT CRP (ICRP)
Immunotherapy
Breast cancer
4T1
Tumor microenvironment
Treatment

ABSTRACT

In 1889, Steven Paget postulated the theory that cancer cells require a permissive environment to grow. This permissive environment is known as the tumor microenvironment (TME) and nowadays it is evident that the TME is involved in the progression and response to therapy of solid cancer tumors. Triple-negative breast cancer is one of the most lethal types of cancer for women worldwide and chemotherapy remains the standard treatment for these patients. IMMUNEPOTENT CRP is a bovine dialyzable leukocyte extract with immunomodulatory and antitumor properties. The combination of chemotherapy and IMMUNEPOTENT CRP improves clinical parameters of breast cancer patients. In the current study, we aimed to evaluate the antitumor effect of doxorubicin/cyclophosphamide chemotherapy plus IMMUNEPOTENT CRP and its impact over the tumor microenvironment in a triple-negative breast cancer murine model. We evaluated $CD8^+$, $CD4^+$, T regulatory cells, memory T cells, myeloid-derived suppressor cells, $CD71^+$, innate effector cells and molecules such as α-SMA, VEGF, CTLA-4, PD-L1, Gal-3, IDO, IL-2, IFN-γ, IL-12, IL-6, MCP-1, and IL-10 as part of the components of the TME. Doxorubicin/cyclophosphamide + IMMUNEPOTENT CRP decreased tumor volume, prolonged survival, increased infiltrating and systemic $CD8^+$ T cells and decreased tumor suppressor molecules (such as PD-L1, Gal-3, and IL-10 among others).

In conclusion, we suggest that IMMUNEPOTENT CRP act as a modifier of the TME and the immune response, potentiating or prolonging anti-tumor effects of doxorubicin/cyclophosphamide in a triple-negative breast cancer murine model.

1. Introduction

Breast cancer is the most common type of cancer and the second most lethal among women worldwide [1,2]. More than 1,000,000 women are diagnosed with breast cancer every year and 410,000 will die from the disease [2]. Some subtypes of the disease, such as triple-negative breast cancer, are particularly aggressive; the average overall survival for patients with this form of cancer is 18 months [3]. These tumors lack estrogen, progesterone, and the human epidermal growth factor 2 receptors, rendering this type of cancer resistant to targeted therapies [4].

Chemotherapy drugs remains the cornerstone treatment for most types of cancer, reducing tumor burden by killing malignant cells; however, drug resistance and toxic side effects lead to disease progression and metastasis [5].

In 1889, Steven Paget stated the "seed and soil" hypothesis where he posited that fertile soil (the microenvironment) is essential for the seed (cancer cells) to grow [6]. The tumor microenvironment (TME) concept highlights the participation of immune system cells, extracellular matrix, stromal cells, cancer cells, and signaling molecules in

Abbreviations: TME, tumor microenvironment; TNBC, triple-negative breast cancer; ICRP, IMMUNEPOTENT CRP; Dox, doxorubicin; Cyclo, cyclophosphamide; MDSC, myeloid-derived suppressor cells

* Corresponding author.
E-mail address: moyfranco@gmail.com (M.A. Franco-Molina).

https://doi.org/10.1016/j.biopha.2020.110062
Received 29 September 2019; Received in revised form 26 February 2020; Accepted 27 February 2020

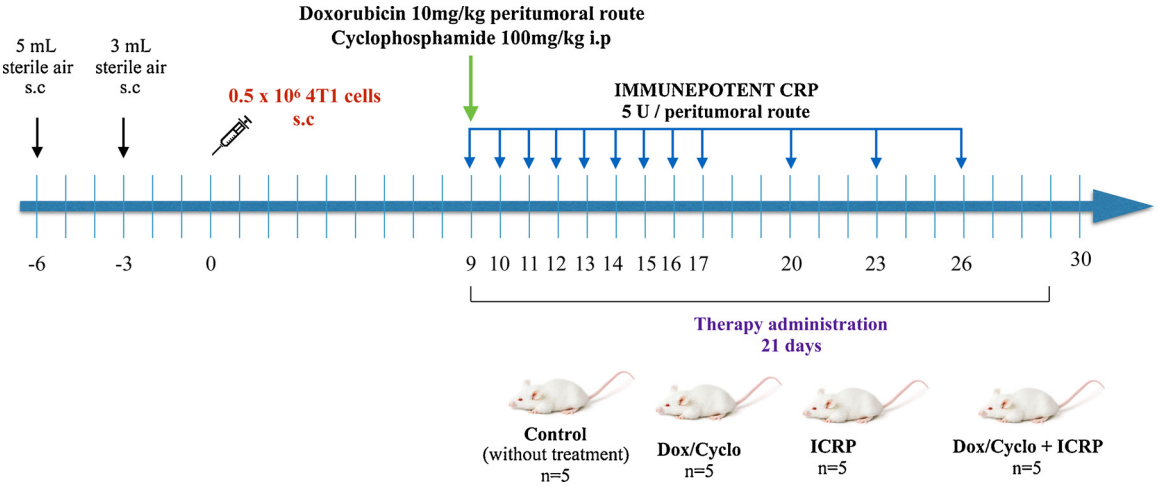

Fig. 1. Air pouch induction, 4T1 cells inoculation and therapy administration.

cancer development and response to oncological treatments [7]. Novel approaches for the management of cancer patients should focus on combined therapies that simultaneously target multiple components of the tumor microenvironment and harness the immune response against cancer cells [8].

IMMUNEPOTENT CRP (ICRP) is an immunomodulator that comprises a mixture of small molecules (> 12KDa) derived from bovine spleen [9]. Our research group has demonstrated that ICRP has several antitumor properties. It decreases inflammation and oxidative stress through NF-κB pathway in murine macrophages *in vitro* [10], induces apoptosis in breast cancer cells [11], decreases myelosuppression in healthy mice treated with the chemotherapy agent 5-fluorouracil [9], induces immunogenic cell death in a murine melanoma model [12], and prevents implantation in a murine lymphoma model [13].

Based on its immunomodulatory properties, we hypothesized that ICRP can be used to modify the tumor microenvironment and increase systemic immunity, thus enhancing the antitumor effect of the doxorubicin/cyclophosphamide treatment in a triple-negative breast cancer murine model.

To assess our hypothesis we evaluated CD8, CD4, T reg, memory T cells, myeloid derived suppressor cells (MDSC), CD71 (transferrin receptor), innate effectors cells (monocytes/macrophages, natural killer cells, granulocytes and dendritic cells) and molecules such as α-smooth muscle actin (SMA), vascular endothelial growth factor (VEGF), cytotoxic T cell ligand associated-4 (CTLA-4), programmed death cell ligand-1 (PDL-1), galectin 3 (Gal-3), indoleamine 2,3-dioxygenase (IDO), IL-2, IFN-γ, IL-12, IL-6, MCP-1, and IL-10 as part of the components of the tumor microenvironment of a 4T1 breast cancer model.

2. Methods

2.1. Cell line

4T1 murine breast cancer cell line was purchased from the American Type Culture Collection (Manassas, Virginia, USA). Cells were cultured in Dulbecco's Modified Eagle Medium (DMEM) supplemented with bovine fetal serum (10 % v/v) in a 37 °C and 5% CO_2 atmosphere.

2.2. Animals

BALB/c female mice (6–8 weeks old) were provided by the bioterium of the Facultad de Ciencias Biológicas, UANL. Mice were kept in 12 h light/dark cycles with *ad libitum* water and food. All animal procedures were performed according to the official Mexican norm of Animal Welfare NOM-033-SAG/ZOO-2014 and approved by the internal Research and Animal Welfare Ethics Committee (CEIBA) of the Facultad de Ciencias Biológicas, UANL.

2.3. Reagents

ICRP is an endotoxin-free dialyzed (> 12 KDa) bovine leukocyte extract. One unit of ICRP has been defined as the product derived from 1×10^8 bovine spleen cells. Doxorubicin (Doxolem®) was purchased from Teva Pharmaceuticals (México). Cyclophosphamide (Hidrofosmin®) was purchased from Sanfer Laboratories (Mexico).

2.4. Air pouch induction, 4T1 cells inoculation, and animal treatments

Tumor cells were inoculated inside an air pouch. The air pouch technique allows for a more accurate assessment by creating a confined/defined environment in which the candidate drug is in direct contact with the tumor [14]. The mice's backs were shaved, and 5 mL of sterile air was injected by subcutaneous route. Three days later, 3 additional mL of sterile air was injected to avoid de-inflation [14].

4T1 viable cells (0.5×10^6) were injected inside the air pouch. Nine days after inoculation, tumors reached approximately 100 mm^3 and mice were randomly divided into four experimental groups (n = 5): 1) control group: without treatment, 2) Dox/Cyclo (doxorubicin/ cyclophosphamide) group: a single dose of Dox (10 mg/kg, peritumoral route) and Cyclo (100 mg/kg, i.p route), 3) ICRP group: 5 units of ICRP daily for 9 days, and 3 more administrations every third day, by peritumoral route and 4) Dox/Cyclo + ICRP: mice received both treatments (Dox/Cyclo + ICRP) as previously described. Sacrifice was performed 30 days after 4T1 cell inoculation. Air pouch induction, 4T1 cell inoculation and treatment administration are depicted in Fig. 1.

Tumor width and length were measured every third day and tumor volume was calculated with the formula: (width^2 x length)/2 [15]. For weight determination, tumors were removed (*postmortem*) and weighed using a TE241S laboratory analytical balance (Sartorius, Goettingen, Germany). Data are presented as the mean ± standard deviation of five animals per group.

For the animal survival experiment, five additional mice per experimental group were kept under observation for 60 days after 4T1 cell inoculation. Mice were sacrificed if tumor volume reached 2000 mm^3. Survival was plotted in a Kaplan-Meier graph.

2.5. Immunohistochemistry

Tumors were dissected and fixed in formalin (10 % in PBS, pH 7.2) for 24 h, followed by paraffin embedding. Tumor sections (3–5 μm) were cut, deparaffinized and hydrated in a xylol-alcohol gradient.

Tumor slides were incubated with 0.3 % H_2O_2 in Tris-buffered saline (TBS) for 5 min and TBS plus 0.025 % Triton X-100 for 5 min. For antigen retrieval, samples were incubated with sodium citrate buffer (10 mM sodium citrate, 0.05 % Tween 20, pH 6.0) for 30 min at 60 °C. Tumor slides were blocked with horse normal serum Vector Laboratories, California, USA. Samples were incubated with the following primary antibodies: anti-CTLA-4 sc-376016, anti-PD1 sc-12767, anti-PD-L1 364568, anti-IDO sc-137012, anti-Gal-3 sc-32790, anti-Ki-67 381308, anti-cleaved-Caspase-3 ab214430, anti-VEGF sc-130289 or anti-SMA A076031D at 4 °C for 24 h. All antibodies were used in a 1:1000 dilution. All antibodies were purchased from Santa Cruz Biotechnology (California, USA) except for anti-Ki-67, anti-SMA, and anti-PD-L1, which were purchased from US Biological (Massachusetts, USA), and anti-cleaved-Caspase-3 which was purchased from Abcam (Missouri, USA). Samples were incubated with biotinylated pan-specific universal secondary antibody (Vector Laboratories, California, USA) for 10 min, counterstained with hematoxylin (Sigma Aldrich, Missouri, USA) for 30 s, dehydrated in a xylol-alcohol gradient and mounted with Entellan® (Merck Millipore, Darmstadt, Germany).

Digital micrographs were captured with a Zeiss Imager.Z1 microscope (Zeiss, Germany) equipped with an AxioCam MRc5 camera (Zeiss, Germany), and using the AxioVision V4.6 (Zeiss, Germany) software.

DAB positive staining is evidenced by brown colored cells. Quantification of staining intensity was performed using the image processing software Fiji (ImageJ version 2.0) as described by Patera et al. [16].

Briefly, the function color deconvolution (histological dyes digital separation) was applied to the microphotographs; this provides three independent digital images (H&E, DAB, and a complementary image), after this stain-specific values for the optical density in each of the three images can be determined. Mean grey values were collected from image 2 (DAB) and optical density was calculated with the formula optical density = log(max grey intensity/mean grey intensity). Data are presented as the mean optical density ± standard deviation of five sections per tumor slide (five slides per group). The average mean optical density was compared between groups.

2.6. Splenocyte isolation

After the sacrifice, the spleens were aseptically removed from the mice and placed on Petri dishes. Splenocytes were flushed out of the spleen with sterile PBS (10 mL), briefly, PBS (10 mL) were injected through each spleen, the PBS-cell suspension was collected, and this step was repeated for 7–10 times or until the organ became pale. After this, the spleen cells-PBS suspension was centrifuged at 1200 rpm for 10 min. To eliminate erythrocytes, the pellet was incubated with sterile erythrocyte lysis solution (0.8 % NH4Cl, 0.1 mM EDTA, pH 7.2–7.6) in mild agitation for 5 min and centrifuged at 1200 rpm for 10 min. Splenocytes were resuspended in DMEM cell culture media. Cell viability and count were determined by the trypan blue exclusion technique. This procedure can yield from 5×10^6 to 13×10^6 viable splenocytes. Differences could be attributable to tumor properties (splenomegaly) or treatment (chemotherapy reduces spleen size).

2.7. Ex vivo splenocyte/4T1 co-culture

Cells (5×10^4 4T1) were seeded in 24 well plates at 37 °C and 5% CO_2 atmosphere for 24 h. Splenocytes from mice without tumor or control tumor-bearing mice (untreated) or treated with Dox/Cyclo, ICRP or Dox/Cyclo + ICRP were added in a 1:1, 1:10 and 1:25 target:effector cell ratio for 24 h at 37 °C and 5% CO_2 atmosphere. 4T1 cells were detached with Accutase (Sigma Aldrich, Missouri, USA). 4T1 cell death was analyzed with 7AAD staining by flow cytometry with a BD Accuri™ C6 flow cytometer (BD Biosciences, California, USA), excluding splenocytes by cell size and granularity. Data are presented as the mean ± standard deviation of five animals per group.

2.8. Cytokines determination

Cytokines were analyzed in serum and tumor tissue at the end of the experiment (30 days after tumor cell inoculation). For tumor tissue samples, tumors were sliced and incubated at 4 °C with lysis buffer (150 mM sodium chloride, 1% triton 100-X, 50 mM Tris, Halt™ Protease Inhibitor Cocktail, pH 8.0) in mild agitation for 60 min. Then lysed tumors were centrifuged for 20 min at 12,000 rpm and the supernatant was collected for further analysis. For serum, peripheral blood was centrifuged at 3600 rpm for 10 min at 4 °C in an Eppendorf 5804R refrigerated centrifuge (Hamburg, Germany).

Cytokine levels were determined with the BD Cytometric Bead Array (CBA) Mouse Inflammation Kit (BD Horizon, California, USA) according to the manufacturer instructions. Briefly, 50 μL of Mouse Inflammation capture beads were mixed with 50 μL of each sample and 50 μL Mouse Inflammation PE Detection Reagent. Assay tubes were incubated for 2 h in the dark at room temperature. After this, 1 mL of wash buffer was added to the assay tubes and centrifuged for 5 min at 1200 rpm. The supernatant was discarded, and the pellet was re-suspended in 100 μL of wash buffer. Events were acquired in a BD Accuri™ C6 flow cytometer (BD Horizon, California, USA). Cytokine levels were analyzed with the CFlow plus software (BD Biosciences, California, USA). Data are presented as the mean ± standard deviation of five animals per group.

2.9. Leukocyte isolation

Tumors were sliced and incubated with 0.1 mg/mL of Liberase™ TL (Roche, Mannheim, Germany) at 37 °C for 30 min in mild agitation. The resulting cell suspension was rinsed with PBS. Leukocytes from this tumor cell suspension or from peripheral blood were purified by gradient density separation with Polymorphoprep™ reagent (Axis Shield, Dundee, United Kingdom) according to the manufacturer instructions.

2.10. Leukocyte immunophenotyping

Leukocytes were stained with the following fluorophore labelled antibodies: anti-mouse CD3 FITC 555274, anti-mouse CD8 PE 553033, anti-mouse CD4 APC 553051, anti-mouse CD44 PE (51-9007324) anti-mouse CD62 L APC (5-9007326), anti-mouse CD45 PerCP 557235, anti-mouse CD71 FITC 553266, anti-mouse CD16/CD32 APC 558636, anti-mouse CD25 PE 12-0251-81, anti-mouse FOXP3 PE-Cy5 15-5773-80A and anti-mouse Ly6G/C 553128 all manufactured by BD Biosciences California, USA.

For FOXP3 staining, cells were fixed with formaldehyde (4% v/v in PBS) for 1 min and then permeabilized with methanol (90 % in PBS) for 30 min on an ice water bath, washed twice with albumin (0.5 % p/v in PBS) and re-suspended in PBS.

Cells were incubated with the antibodies for 30 min in the dark at room temperature, then centrifuged twice with albumin (0.5 % p/v in PBS) for 5 min at 1200 rpm and resuspended in PBS (100 μL). Events were acquired in a BD Accuri™ C6 flow cytometer (BD Horizon, California, USA). Data are presented as the mean ± standard deviation of five animals per group.

2.11. Hematoxylin and eosin staining

Mice brain, lungs, heart, liver, and spleen were removed and fixed in formalin (10 % in PBS, pH 7.2) for 24 h, followed by paraffin embedding. Tumor sections (3–5 μm) were cut, deparaffinized and hydrated in a xylol-alcohol gradient. Organ tissues were stained with Mayer hematoxylin solution for 8 min and counterstained with eosin-phloxine B solution for 45 s, dehydrated in a xylol-alcohol gradient and mounted with Entellan® (Merck Millipore, Darmstadt, Germany).

2.12. Blood and serum analyses

After sacrifice, blood from all experimental groups was collected in microtainer collection tubes with K_2EDTA for blood analysis and lithium-heparin and gel for serum analysis. Hematological parameters were determined with the Sysmex XS 1000 analyzer (Sysmex, Kobe, Japan) and biochemical parameters with the COBAS INTEGRA® 400 plus analyzer (Roche, Mannheim, Germany). Data are presented as the mean ± standard deviation of five animals per group.

2.13. Statistical analysis

Statistical differences between groups were analyzed using ANOVA followed by the Tukey post-hoc test or Mantle-Cox test (for survival analysis). Differences between groups were considered significant at a p-value ≤ 0.05. Statistical analyses were performed with the GraphPad Prism 7.0 (GraphPad Software, Inc., San Diego, CA).

3. Results

3.1. Dox/Cyclo + ICRP decreased tumor volume and weight and increased animal survival in 4T1-tumor-bearing mice

All treatments significantly reduced (p ≤ 0.05) tumor volume (since day 21) and weight (day 30) (p ≤ 0.05), as compared to the control group (Fig. 2a and b). There was no statistical difference between tumor volumes and weight for the Dox/Cyclo and ICRP treated groups. On the other hand, there was a significant decrease in tumor volume and weight (p ≤ 0.05) after Dox/Cyclo + ICRP treatment compared with the remaining treatments (Fig. 2a and b).

All treatments significantly prolonged (p ≤ 0.001) the survival of tumor-bearing mice compared to the control group (Fig. 2c).

3.2. Dox/Cyclo + ICRP decreased Ki-67 and increased caspase 3

All treatments significantly decreased (p ≤ 0.05) Ki-67 expression as compared to the control group. There was no significant difference (p ≤ 0.05) of Ki-67 expression between treated groups: Dox/Cyclo, ICRP and Dox/Cyclo + ICRP (Fig. 3a and b). Dox/Cyclo + ICRP treatment significantly increased (p ≤ 0.05) caspase-3 expression as compared to the control and Dox/Cyclo groups. There is no statistical difference (p ≤ 0.05) between caspase-3 expression of ICRP and the other groups (Fig. 3a and b).

3.3. Dox/Cyclo + ICRP decreased CTLA-4 and PD-L1

Dox/Cyclo significantly increased (p ≤ 0.05) CTLA-4 expression as compared to the control and Dox/Cyclo + ICRP groups. There was no significant difference (p ≤ 0.05) between CTLA-4 expression in the ICRP group as compared to the others (Fig. 4a and d).

There was no significant difference (p ≤ 0.05) in PD1 expression between groups (Fig. 4b and d).

PD-L1 expression significantly decreased (p ≤ 0.05) in the ICRP and Dox/Cyclo + ICRP treated groups as compared to the control and Dox/Cyclo groups (Fig. 4c and d).

3.4. Dox/Cyclo + ICRP decreased suppressor molecule Gal-3

ICRP significantly decreased (p ≤ 0.05) IDO expression in tumor tissue as compared to the control and Dox/Cyclo groups (Fig. 5a and b). There was no significant difference (p ≤ 0.05) between IDO expression in the Dox/Cyclo + ICRP group as compared to the other groups (Fig. 5a and b).

ICRP and Dox/Cyclo + ICRP treatments significantly decreased (p ≤ 0.05) Gal-3 expression in the tumor as compared to the control and Dox/Cyclo groups (Fig. 5c and d).

3.5. Dox/Cyclo + ICRP decreased VEGF and α-SMA

Dox/Cyclo + ICRP significantly decreased (p ≤ 0.05) VEGF expression as compared to the control, Dox/Cyclo and ICRP groups (Fig. 6a and b).

ICRP and Dox/Cyclo + ICRP significantly decreased (p ≤ 0.05) α-SMA expression as compared to the control and Dox/Cyclo groups (Fig. 6c and d).

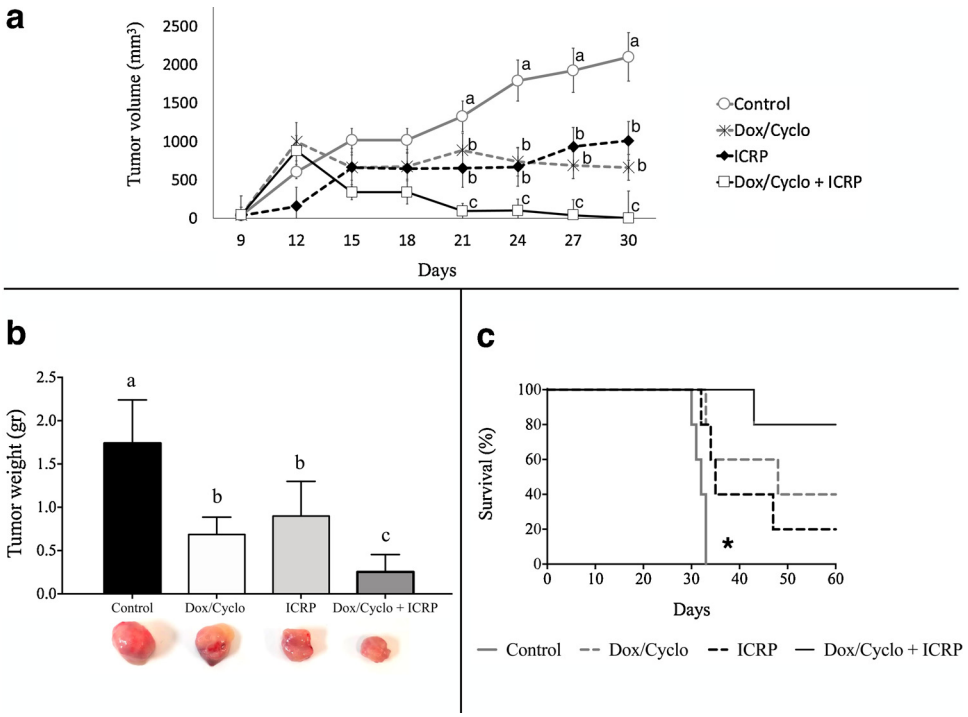

Fig. 2. Tumor volume (a), tumor weight (b) and animal survival (c). (a) Tumor volume (mm^3) was measured every third day since day 9 post inoculation. (b) Thirty days after 4T1 cell inoculation, 5 mice of each experimental group were sacrificed, and the tumor mass was removed and weighted. All data shown represents the mean ± SD. Statistical significance (p ≤ 0.05) was determined by one-way ANOVA and the Tukey post hoc test. There is no statistical difference between bars labeled with the same letter in the graph (^{a,b,c}). (c) Five additional mice per group, were kept for 60 days to plot Kaplan Meier survival curves. Statistical difference between experimental groups (*p ≤ 0.01) was determined with the log-rank test (Mantel-Cox).

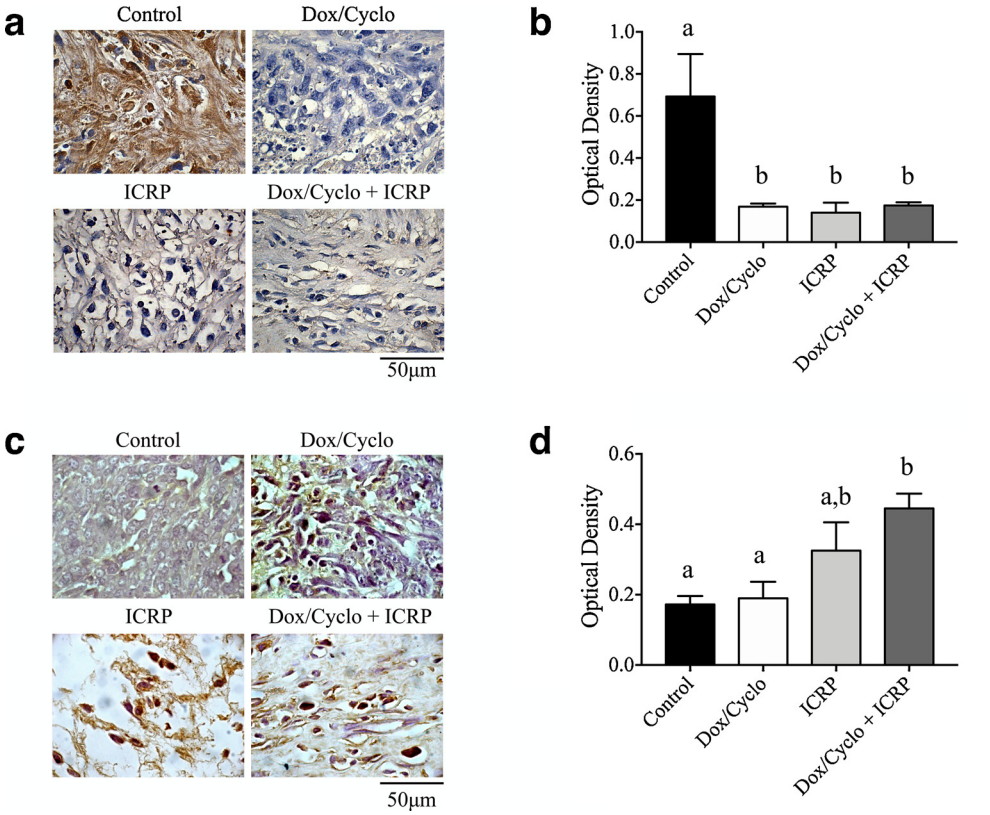

Fig. 3. Immunohistochemical staining and optical density (OD) value of Ki-67 and Caspase-3 in tumor tissue. (a) Representative micrograph of Ki-67 immunostaining visualized with DAB and counterstained with hematoxylin and (b) optical density (mean gray value) obtained by color deconvolution analysis. (c) Representative micrograph of cleaved caspase-3 immunostaining visualized with DAB and counterstained with hematoxylin and (d) optical density (mean gray value) obtained by color deconvolution analysis.
Optical density graph bars (b and d) represent the mean ± SD (n = 5). Statistical significance ($p \leq 0.05$) was determined by one-way ANOVA and the Tukey post hoc test. There is no statistical difference between bars labeled with the same letter in the graph (^{a,b}).

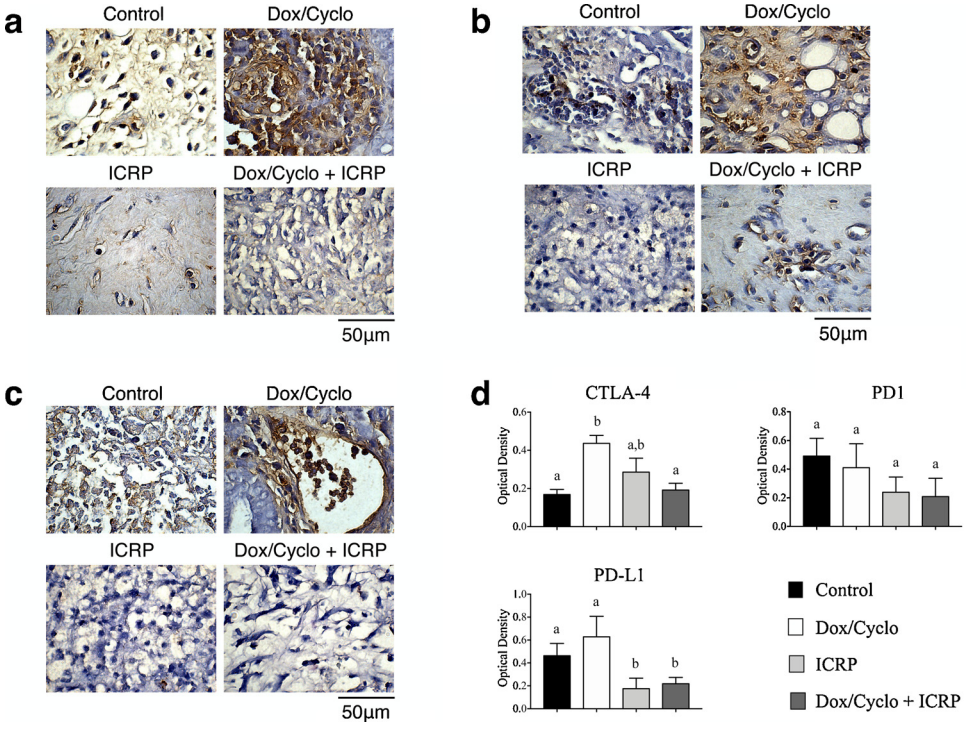

Fig. 4. Immunohistochemical staining and optical density (OD) value of CTLA-4, PD1, and PD-L1 in tumor tissue. Representative micrograph of CTLA-4 (a), PD1 (b), and PD-L1 (c) immunostaining visualized with DAB and counterstained with hematoxylin. (d) Optical density (mean gray value) obtained by color deconvolution analysis. Optical density graph bars represent the mean ± SD (n = 5). Statistical significance ($p \leq 0.05$) was determined by one-way ANOVA and the Tukey post hoc test. There is no statistical difference between bars labeled with the same letter in the graph (^{a,b}).

3.6. ICRP partially restores splenocytes cytotoxic activity in tumor-bearing mice treated with Dox/Cyclo

Viable splenocytes were obtained from mice without tumor and from untreated tumor-bearing mice (control) or treated with Dox/Cyclo, ICRP or Dox/Cyclo + ICRP. Splenocytes (effector cells) were co-cultured with 4T1 cells (target cells) in a 1:1, 1:10 and 1:25 target:effector cell ratio for 24 h.

In the 1:1 ratio, the cytotoxic effect from splenocytes over 4T1 cells was 10 % or less for all tested groups (Fig. 7c).

In the 1:10 ratio, the cytotoxic effect of splenocytes from untreated (23.53 %), ICRP (22.8 %), or Dox/Cyclo + ICRP (21.6 %) tumor-bearing mice was significantly higher ($p \leq 0.05$) than the effect of splenocytes in mice without tumor (1.17 %) and tumor-bearing mice

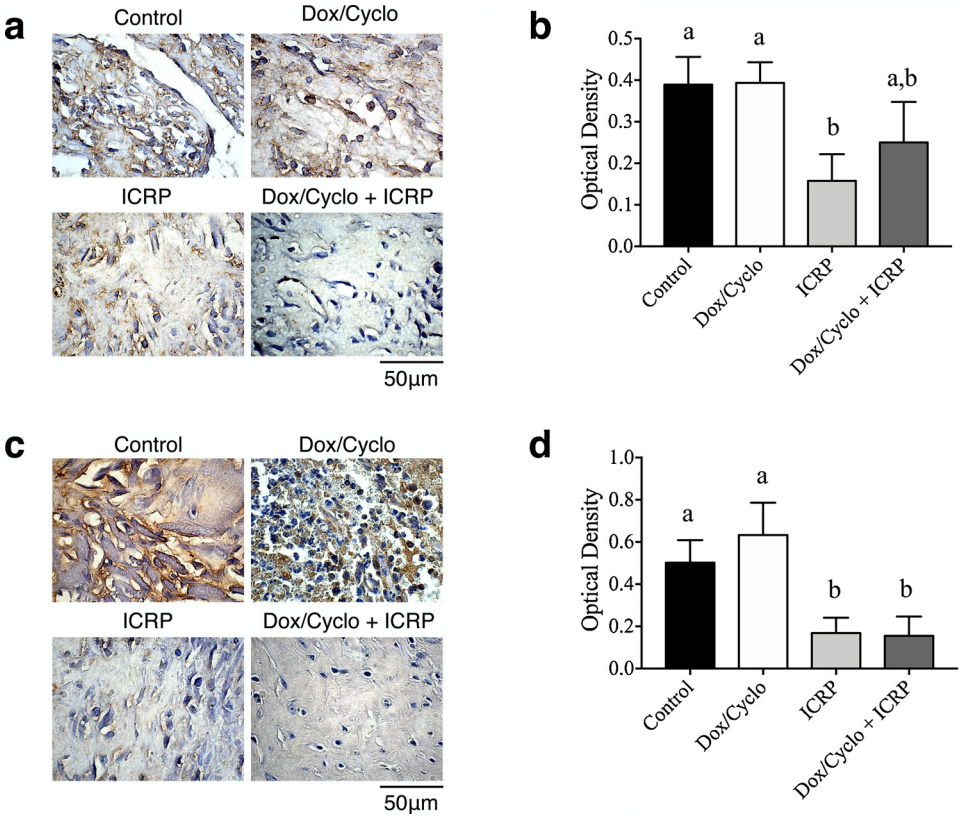

Fig. 5. Immunohistochemical staining and optical density (OD) value of IDO and Gal-3 in tumor tissue. (a) Representative micrograph of IDO immunostaining visualized with DAB and counterstained with hematoxylin and (b) optical density (mean gray value) obtained by color deconvolution analysis. (c) Representative micrograph of galectin 3 immunostaining visualized with DAB and counterstained with hematoxylin and (d) optical density (mean gray value) obtained by color deconvolution analysis. Optical density graph bars (b and d) represent the mean ± SD (n = 5). Statistical significance ($p \leq 0.05$) was determined by one-way ANOVA and the Tukey post hoc test. There is no statistical difference between bars labeled with the same letter in the graph ([a,b]).

treated with Dox/Cyclo (5.83 %). There was no statistical difference ($p \leq 0.05$) between the cytotoxic effect of splenocytes from mice without tumor and tumor-bearing mice treated with Dox/Cyclo (Fig. 7c).

In the 1:25 ratio, the cytotoxic effect of splenocytes from untreated (67.03 %), ICRP (56.2 %), or Dox/Cyclo + ICRP (41.07 %) tumor-bearing mice was significantly higher ($p \leq 0.05$) than the effect of splenocytes of mice without tumor (12.6 %) and tumor-bearing mice treated with Dox/Cyclo (11.97 %). The cytotoxic effect of splenocytes

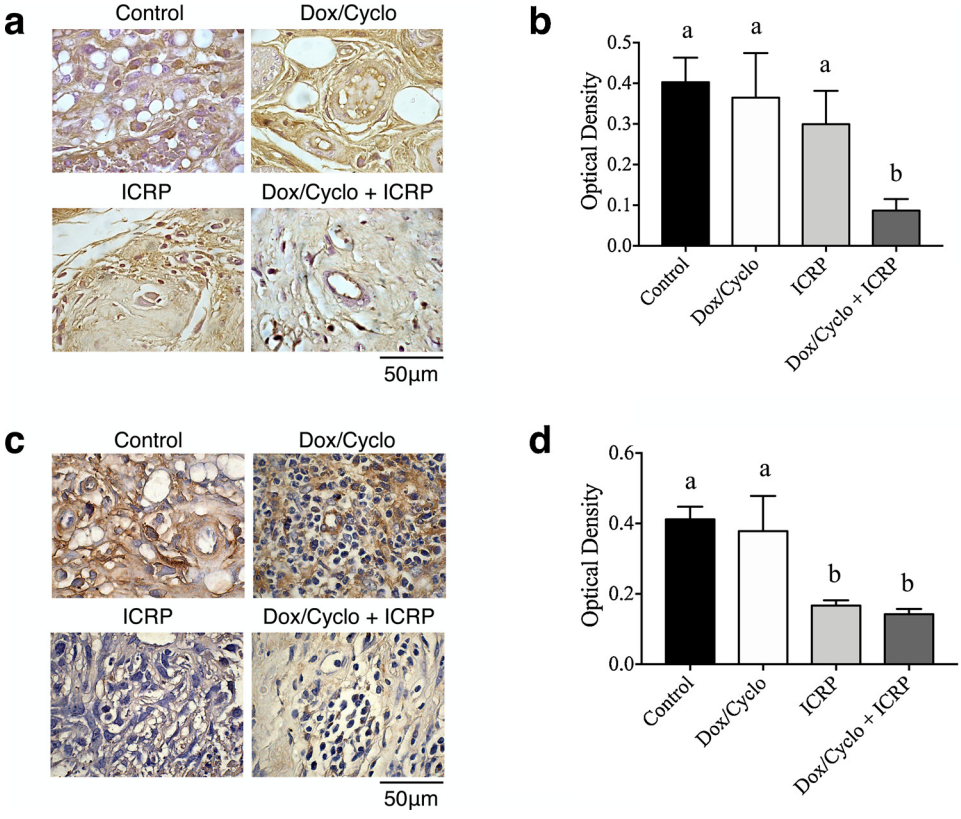

Fig. 6. Immunohistochemical staining and optical density (OD) value of VEGF and α-SMA in tumor tissue. (a) Representative micrograph of VEGF immunostaining visualized with DAB and counterstained with hematoxylin and (b) optical density (mean gray value) obtained by color deconvolution analysis. (c) Representative micrograph of α-SMA immunostaining visualized with DAB and counterstained with hematoxylin and (d) optical density (mean gray value) obtained by color deconvolution analysis. Optical density graph bars (b and d) represent the mean ± SD (n = 5). Statistical significance ($p \leq 0.05$) was determined by one-way ANOVA and the Tukey post hoc test. There is no statistical difference between bars labeled with the same letter in the graph ([a,b]).

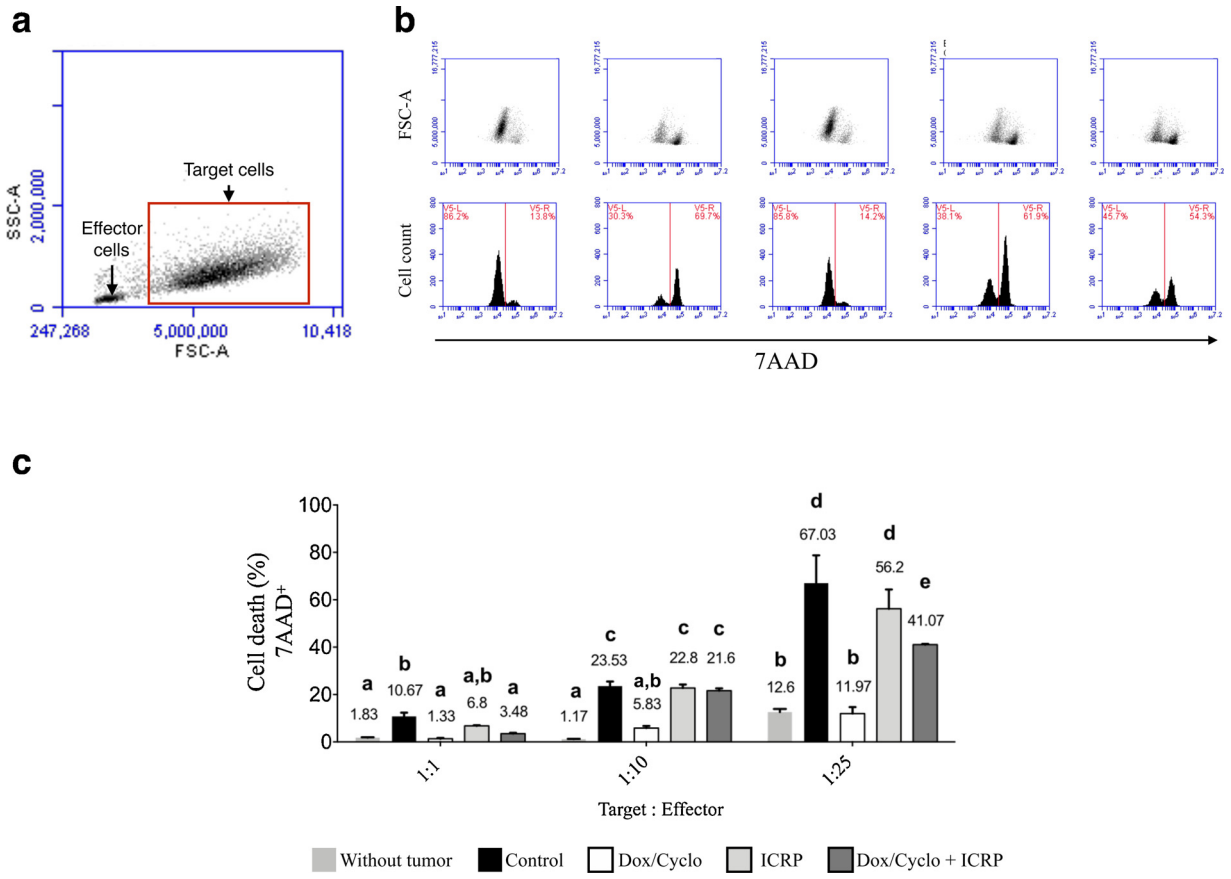

Fig. 7. *Ex-vivo* cytotoxic effect of splenocytes over 4T1 cells. Splenocytes from mice without tumor and untreated 4T1 tumor-bearing mice or treated with: Dox/Cyclo, ICRP, or Dox/Cyclo + ICRP were co-cultured with 5 × 10^4 4T1 cells for 24 h. The figure shows representative dot plot of the FSC (size) and SSC (granularity) gating strategy to discriminate splenocyte (effector cells) and 4T1 (target cells) (a); FSC dot plot and cell count histogram *versus* 7AAD staining for the 1:25 target/effector cell ratio (b); and cell death (%) graph bars representing 7AAD positive staining in the target/effector cell ratio 1:1, 1:10, and 1:25. Graph bar values represent mean ranges ± SD ($p \leq 0.05$) (n = 5). Statistical significance was determined by the Tukey post hoc test. There is no statistical difference between bars labeled with the same letter in the graph (^{a,b,c,d}).

from untreated mice or mice treated with ICRP was significantly higher ($p \leq 0.05$) than the cytotoxic effect of splenocytes from Dox/Cyclo + ICRP treated mice (Fig. 7b and c).

3.7. Dox/Cyclo + ICRP increased TNF-α, IFN-γ, IL-12, IL-6, MCP-1 and IL-10 serum levels

All treatments significantly increased ($p \leq 0.05$) IFN-γ, IL-12, IL-6, IL-10 and MCP-1 in sera as compared to the control. Dox/Cyclo + ICRP significantly increased ($p \leq 0.05$) TNF-α (70.27 pg/mL) when compared to the control (41.34 pg/mL). There was no significant difference ($p \leq 0.05$) for TNF-α, IFN-γ and IL-6 expression between treated groups, however, significant difference ($p \leq 0.05$) was found for IL-12 and IL-10 (Fig. 8).

3.8. Dox/Cyclo + ICRP increased IFN-γ levels in tumor tissue

At the level of tumor microenvironment, Dox/Cyclo + ICRP significantly increased ($p \leq 0.05$) TNF-α, IFN-γ and IL-6 levels and significantly decreased ($p \leq 0.05$) IL-10 as compared to the control group (Fig. 9).

ICRP significantly increased ($p \leq 0.05$) IFN-γ (2.54 pg/mL) and IL-12 (61.85 pg/mL), and significantly decreased ($p \leq 0.05$) IL-6 (15.88 pg/mL), IL-10 (86.08 pg/mL) and MCP-1 (139.67 pg/mL) cytokines, without affecting TNF-α (14.06 pg/mL), when compared to the control (Fig. 9).

Dox/Cyclo treatment did not affect the evaluated cytokines as compared to the control, except for IL-6 (10.33 pg/mL), that significantly decreased ($p \leq 0.05$) (Fig. 9).

3.9. Dox/Cyclo + ICRP increased cytotoxic and memory T cells and decreased T regulatory lymphocytes and myeloid suppressor cells in peripheral blood of 4T1 tumor-bearing mice

Dox/Cyclo significantly increased ($p \leq 0.05$) CD8 (51 %) and T reg cells (73 %) and significantly decreased ($p \leq 0.05$) innate effector cells (9.35 %) without affecting CD4 (58.4 %), memory T cells (32.65 %), CD71 (28.05 %), and MDSC (29 %) populations as compared to the control.

ICRP significantly increased ($p \leq 0.05$) CD8 (96.6 %), memory T cells (71.95 %), innate effector cells (45.7 %) and decreased significantly ($p \leq 0.05$) CD4 (16.95 %) without affecting CD71 (41.24 %), T reg (29.75 %) and MDSC (24.05 %) as compared to the control.

Dox/Cyclo + ICRP significantly increased ($p \leq 0.05$) CD8 (66.95 %), memory T cells (71.65 %), and T reg (46.9 %) and significantly decreased ($p \leq 0.05$) CD4 (33.05 %), MDSC (13.2 %) without affecting CD71 (13.25 %) and innate effector cells (31.2 %) as compared to the control.

When compared between treated groups, ICRP, as monotherapy and combined, significantly increased ($p \leq 0.05$) CD8 (96.6 % and 66.95 %) and memory T cells (71.95 % and 71.54 %) compared to the Dox/Cyclo group (51 % and 32.65 %, respectively). Also, ICRP, as monotherapy and combined, decreased T reg (29.75 % and 46.9 %, respectively) as compared with Dox/Cyclo (73 %).

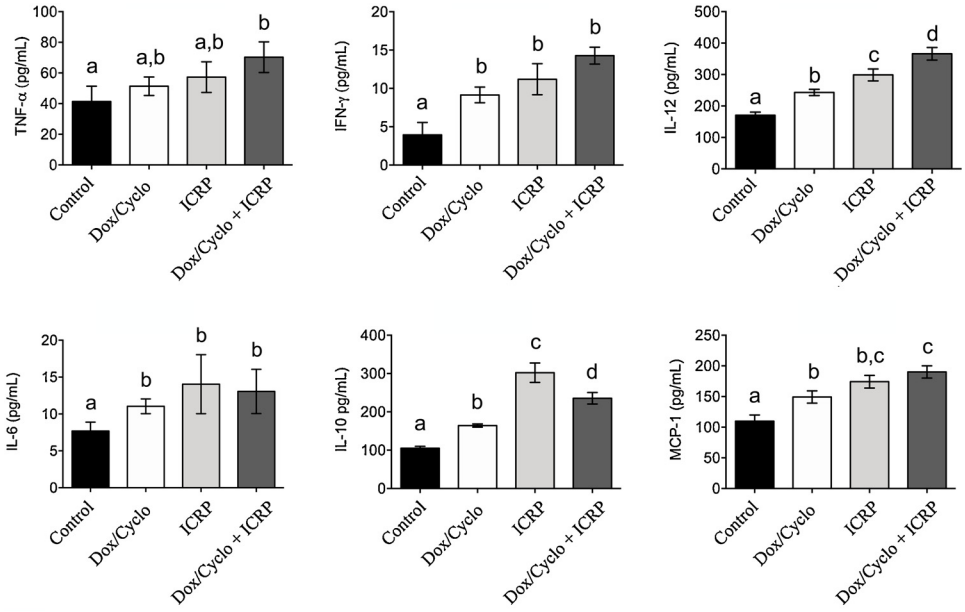

Fig. 8. TNF-α, IFN-γ, IL-12, IL-6, IL-10, and MCP-1 levels in serum. 30 days after 4T1 cell inoculation, serum was collected from untreated 4T1 tumor-bearing mice (control) or treated with: Dox/Cyclo, ICRP, or Dox/Cyclo + ICRP. Graph bars represent cytokine levels determined by flow cytometry analysis with the CBA mouse inflammation kit. Data is expressed as mean values ± SD ($p \leq 0.05$) (n = 5). Statistical significance was determined by the Tukey post hoc test. There is no statistical difference between bars labeled with the same letter in each graph ([a,b,c,d]).

Dox/Cyclo + ICRP significantly decreased ($p \leq 0.05$) CD71 (13.25 %) as compared to the Dox/Cyclo group (28.05 %).

ICRP significantly increased ($p \leq 0.05$) innate effector cells (45.7 %) as compared to the other groups (Fig. 10).

3.10. Dox/Cyclo + ICRP increased cytotoxic and memory T cells, and innate effector cells in tumor tissue

Dox/Cyclo + ICRP significantly increased ($p \leq 0.05$) CD8 cells (93.5 %) as compared to all other groups.

Dox/Cyclo + ICRP significantly increased ($p \leq 0.05$) memory T cells (85.1 %) as compared to the control group (32.65 %) and significantly decreased ($p \leq 0.05$) T regulatory cells (14.2 %) as compared to the control group (52.95 %).

ICRP and Dox/Cyclo + ICRP significantly increased ($p \leq 0.05$) innate effector cells (45.35 % and 49.8 %, respectively) as compared to control (12.75 %) and Dox/Cyclo (27.85 %) groups.

ICRP and Dox/Cyclo + ICRP significantly decreased ($p \leq 0.05$) MDSC (28.3 % and 3.2 %, respectively) as compared to the Dox/Cyclo group (59.9 %) (Fig. 11).

3.11. ICRP and Dox/Cyclo + ICRP did not affect tissue histology of spleen, liver, kidney, brain, lung and heart of 4T1 tumor-bearing mice

Hematoxylin and eosin (H&E) stain revealed no noticeable damage or inflammatory lesions in major organs (spleen, liver, kidney, brain, lung and heart) for any experimental group (Fig. 12).

3.12. ICRP and Dox/Cyclo + ICRP improved hematological and biochemical parameters in 4T1 tumor-bearing mice

Hematological parameters were in the standard range, except for leukocytosis in the control (15.21 ± 1.62 10^9 x L) (Table 1). Serum biochemical parameters were also in the standard range, except for aspartate aminotransferase and alanine aminotransferase which increased in the control (276.5 ± 20 UI/L and 187 ± 25 U/L,

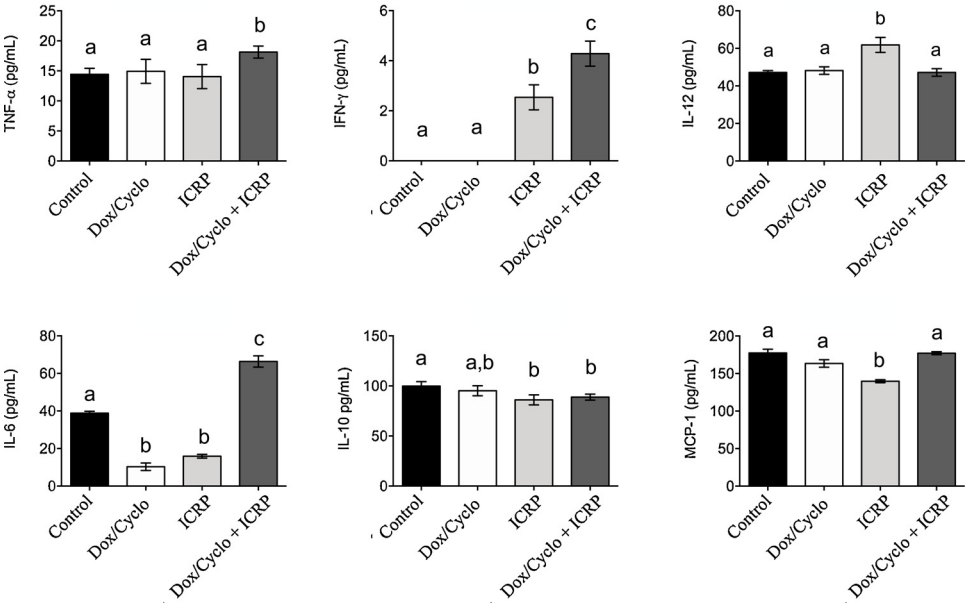

Fig. 9. TNF-α, IFN-γ, IL-12, IL-6, IL-10, and MCP-1 levels in tumor tissue. 30 days after 4T1 cell inoculation, untreated 4T1 tumor-bearing mice (control) or treated with: Dox/Cyclo, ICRP, or Dox/Cyclo + ICRP were sacrificed and had their tumors removed. Tumors were disaggregated with Liberase™ TL and centrifuged to obtain the supernatant. Graph bars represent cytokine levels determined by flow cytometry analysis with the CBA mouse inflammation kit. Data is expressed as mean values ± SD ($p \leq 0.05$) (n = 5). Statistical significance was determined by the Tukey post hoc test. There is no statistical difference between bars labeled with the same letter in each graph ([a,b,c,d]).

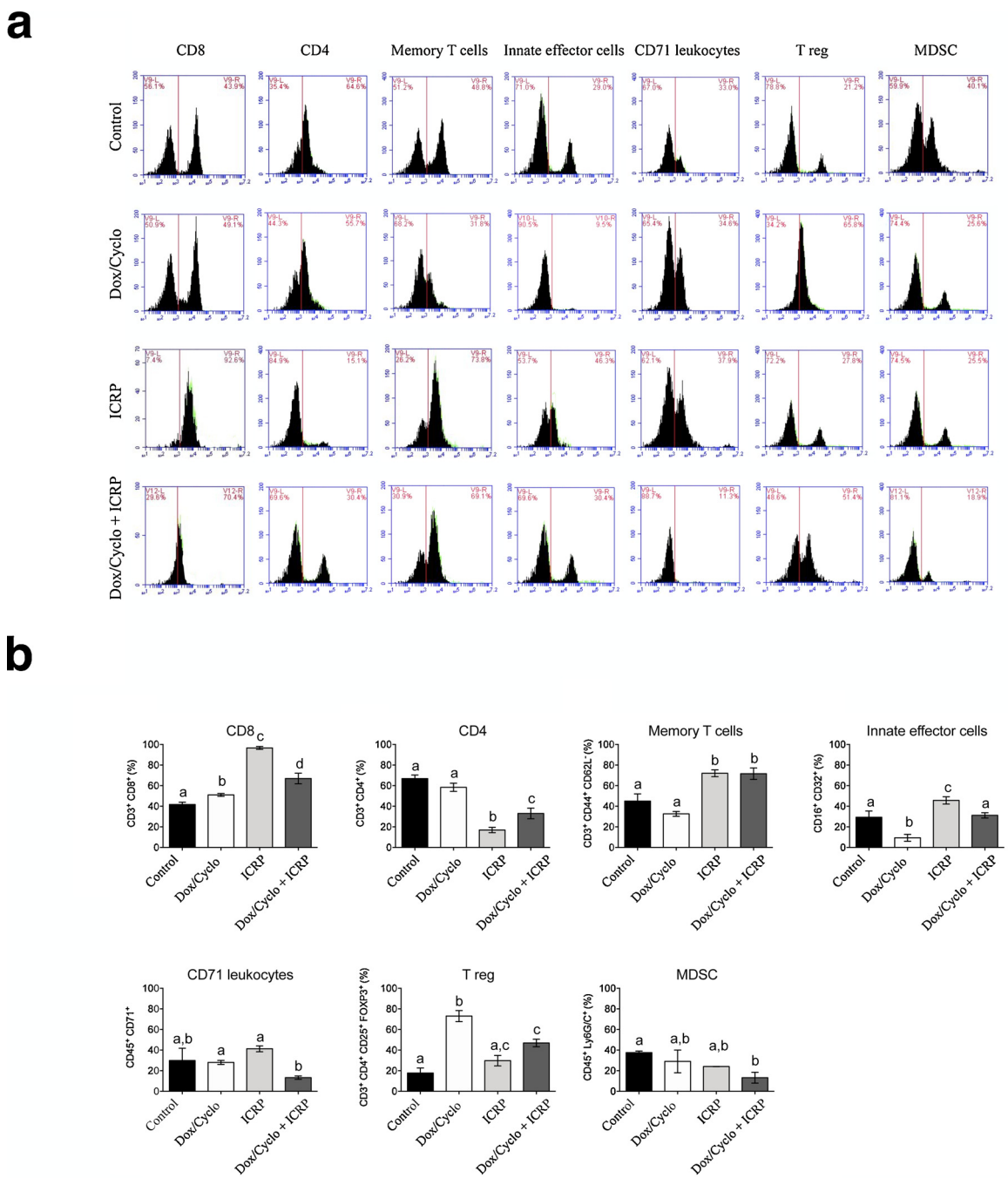

Fig. 10. Immunophenotype of peripheral blood leukocytes. Blood was taken from untreated 4T1 tumor-bearing mice (control) or treated with: Dox/Cyclo, ICRP, or Dox/Cyclo + ICRP 30 days after 4T1 cell inoculation. The figure shows (a) histograms representing the percentage of CD8, CD4, memory T cells, CD71 leukocytes cells, innate effector cells, T reg and MDSC *versus* cell count in the Y axis. And (b) bar graphs representing the mean percentage per group (n = 5) ± SD ($p \leq 0.05$) for each phenotype, as determined by flow cytometry. Statistical significance was determined by the Tukey post hoc test. There is no statistical difference between bars labeled with the same letter in each graph (^{a,b,c,d}).

respectively) and their levels were partially restored in the Dox/Cyclo (97 ± 1.41 UI/L and 59.5 ± 0.71 U/L, respectively), ICRP (152 ± 59.4 UI/L and 90.5 ± 40.31 U/L, respectively) and Dox/Cyclo + ICRP (98 ± 2.83 UI/L and 56 ± 8.49 U/L, respectively) groups (Table 2).

4. Discussion

Our results showed that all treatments delayed tumor growth and increased mice survival; however, the combined therapy was more effective than Dox/Cyclo or ICRP alone. Although chemotherapy induces systemic immunosuppression, it can also work with immunotherapies by decreasing tumor-induced local immunosuppression through cancer cell debulking, potentiating the antitumor effect of combined therapies [17].

All treatments decreased Ki-67 expression, but only ICRP and Dox/Cyclo + ICRP treatments increased cleaved caspase-3 expression, correlating with the tumor volume reduction and survival, suggesting that tumor proliferation is reduced. Ki-67 is a cell proliferation marker, and caspase-3 is an enzyme that activates (cleaved) when cells undergo apoptosis [18]. Cancer cells rely on increased proliferation rate and apoptosis resistance to stay alive; drugs or treatments that decrease cell proliferation and restore apoptosis have a potential antitumor effect

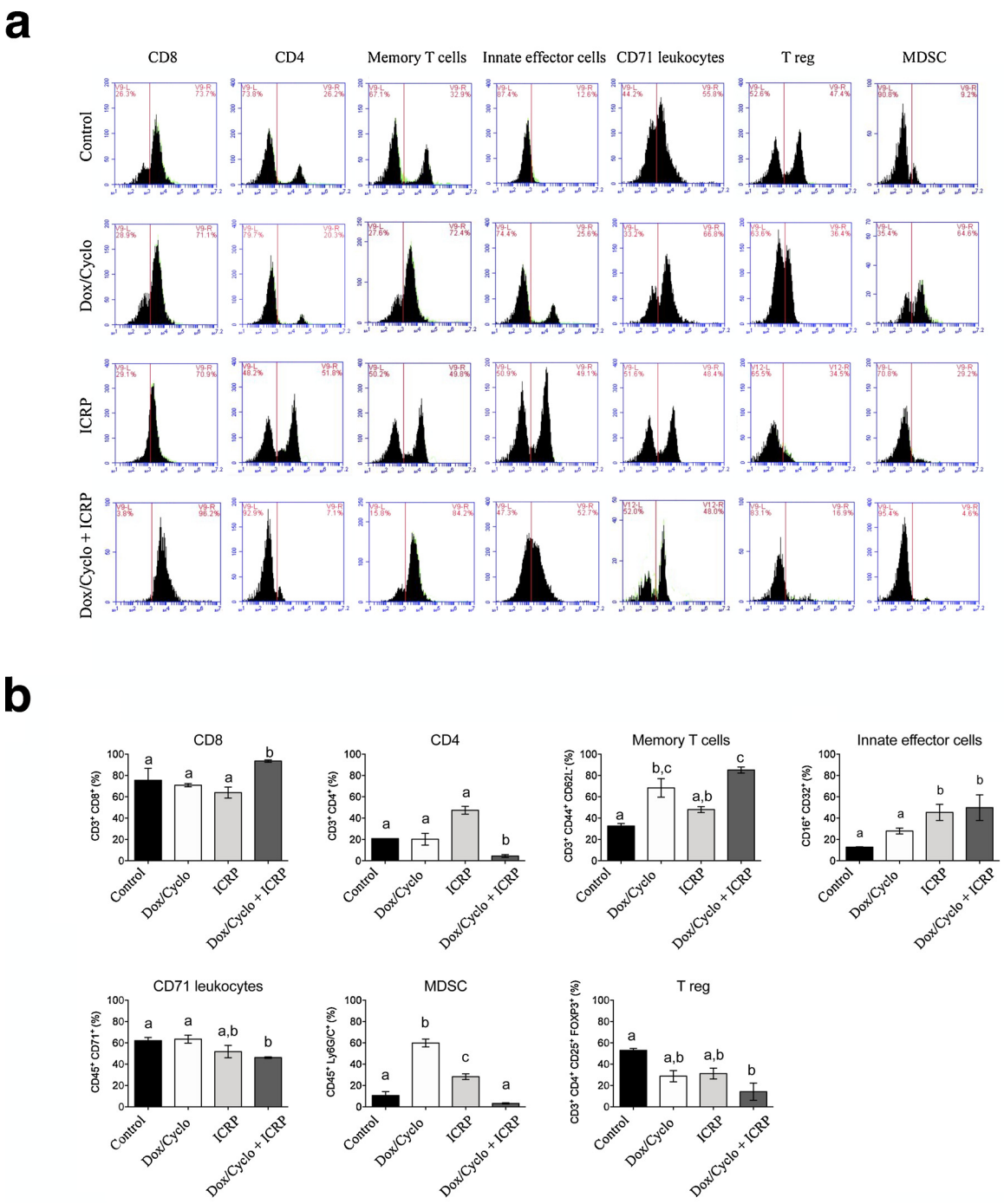

Fig. 11. Immunophenotype of tumor tissue leukocytes. 30 days after 4T1 cell inoculation, untreated 4T1 tumor-bearing mice (control) or treated with: Dox/Cyclo, ICRP, or Dox/Cyclo + ICRP were sacrificed and had their tumors removed. Tumors were disaggregated with Liberase™ TL and leukocytes were isolated by density gradient separation with Polymorphprep™. The figure shows (a) histograms representing the percentage of CD8, CD4, memory T cells, CD71 leukocytes cells, innate effector cells, T reg and MDSC *versus* cell count in the Y axis. And (b) bar graphs representing the mean percentage per group ($n = 5$) ± SD ($p \leq 0.05$) for each phenotype, as determined by flow cytometry. Statistical significance was determined by the Tukey post hoc test. There is no statistical difference between bars labeled with the same letter in each graph (^{a,b,c}).

[19].

Furthermore, the Dox/Cyclo and ICRP combination decreased VEGF and α-SMA expression in the tumor, both of which are desirable targets for cancer therapy [20]. VEGF is a key regulatory of angiogenesis secreted by cancer-associated fibroblasts (CAFs) [20]. α-SMA is used as a marker for CAFs [20]. Tumors require the formation of new blood vessels, mainly induced by CAFs, to obtain oxygen and nutrients [21].

ICRP simultaneously decreased PD-L1, IDO, and Gal-3; however, there was no difference in CTLA-4 and PD1 expression in response to any of the treatments with ICRP. The immune system plays a major role in treatment response and patient outcome; immune cells eliminate drug-resistant cancer cells, and continue to eliminate any emerging tumor cells, even after therapy (immunological memory) [22]. Suppressor immune checkpoints (CTLA-4, PD1, and PD-L1) and molecules (IDO and Gal-3) are overexpressed within the tumor microenvironment, impairing the T cell response and correlating with poor patient outcome [23]. There are previous reports of compounds that modulate immune checkpoints and suppressor molecules, for example, curcumin, a

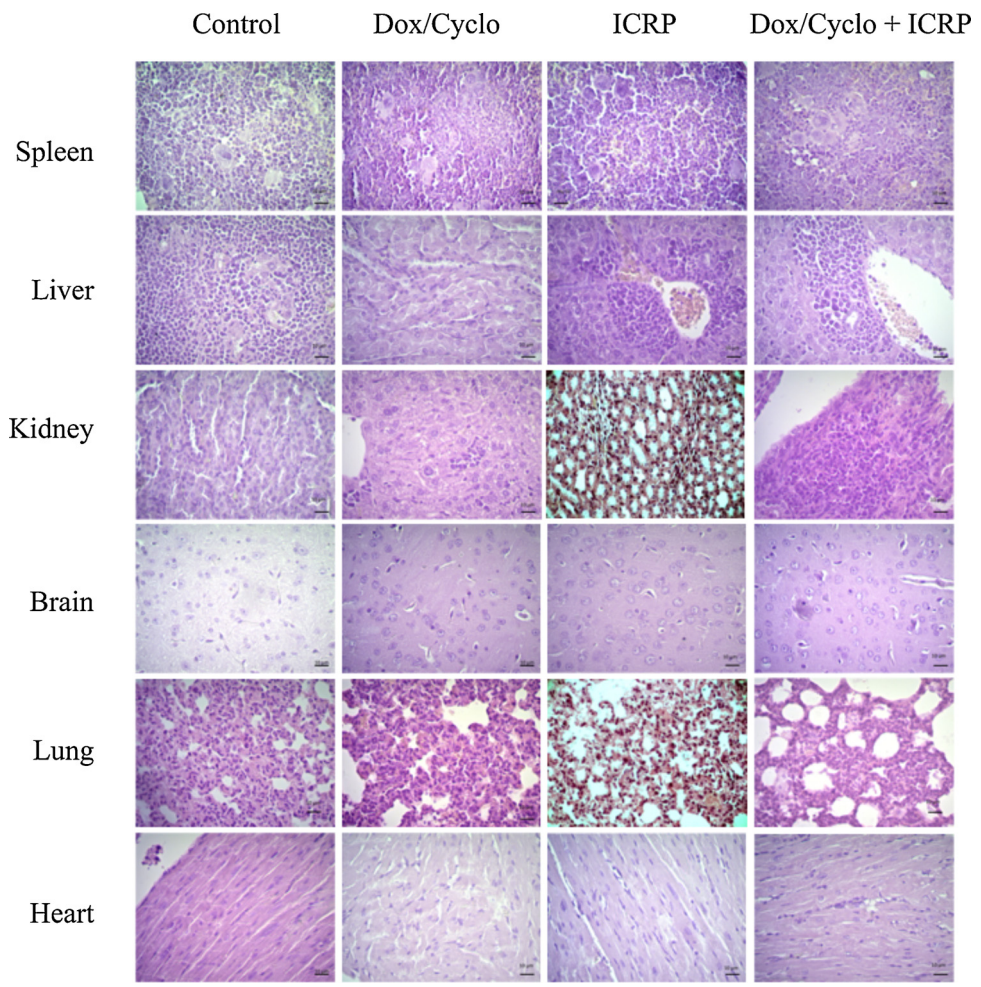

Fig. 12. Representative micrographs of liver, kidney, spleen, heart, lung and brain. Untreated 4T1 tumor-bearing mice or treated with: Dox/Cyclo, ICRP, or Dox/Cyclo + ICRP were sacrificed 30 days after tumor induction. Liver, kidney, spleen, heart, lung and brain were collected and fixed in formaldehyde (10 % v/v), embedded in paraffin, and 5 μm slices were stained with hematoxylin and eosin. Photomicrographs were taken at a magnification x400.

polyphenol derived from the rhizome of *Curcuma longa*, decreases IDO levels in LPS stimulated dendritic cells [24]. Another case is apigenin, which suppresses PD-L1 expression in melanoma and host dendritic cells to elicit synergistic therapeutic effects [25]. CTLA-4 and PD1 are T cell surface receptors that block T cell receptor (TCR) complex activation signals [26]. CTLA-4 and PD1 molecules are mainly expressed by activated T lymphocytes and T reg cells [27], whereas PD-L1, Gal-3 and IDO are expressed not only by T cells, but also by antigen-presenting cells, cancer and stromal cells [28–30], suggesting that ICRP decreases suppression molecules in one or more of these cell types, thus modifying the tumor microenvironment and peripheral immunity to generate an antitumor T cell response.

In order to assess the immunological state of the mice included in this study, we evaluated cytokine profiles and leukocyte markers. All treatments increased systemic IFN-γ, IL-12, and MCP-1, correlating with a T cell 1 ($CD8^+$ T cells that secrete IFN-γ) type immune response. IL-6 and IL-10 serum levels were also increased by all treatments. IL-6 is a pleiotropic pro-inflammatory cytokine associated with inflammation and tumor growth. Despite this, in TNBC models the increase of IL-6 correlates with tumor reduction [31]. IL-10 is classified as an immune-suppressor cytokine, however, it is essential to reduce tumor-associated inflammation, and it is positively correlated with disease-free survival in breast cancer patients [31].

Within the tumor tissue, pro-inflammatory cytokines levels were

Table 1
Hematological parameters of tumor-bearing mice.

	Control	Dox/Cyclo	ICRP	Dox/Cyclo + ICRP	Normal range
Neutrophils (%)	39.5 ± 12.02	42.00 ± 16.97	37.50 ± 9.19	44.50 ± 19.09	35.0–75.0
Lymphocytes (%)	52 ± 8.49	44.50 ± 9.19	52.00 ± 11.31	45.5 ± 7.68	25.0–50.0
Monocytes (%)	7.5 ± 3.54	6.5 ± 3.36	7.50 ± 3.54	7.00 ± 0.01	2.0–10.0
Eosinophils (%)	1 ± 0.5	7.00 ± 1.41	3.00 ± 1.41	3.00 ± 1.41	1.0–4.0
Total white blood cell count (10^9/L)	15.21 ± 1.62[a]	6.49 ± 0.18[b]	9.08 ± 4.24[c]	6.11 ± 3.54[b]	4.00–10.00
Hematocrit (%)	33.95 ± 2.33	40.45 ± 0.49	42.05 ± 3.61	39.15 ± 2.19	40.0–54.0
Hemoglobin (g/dL)	10.95 ± 0.92	12.70 ± 0.5	13.10 ± 1.27	12.05 ± 0.64	14.0–17.5

After 4T1 cell inoculation (day 30), peripheral blood was collected from untreated 4T1 tumor-bearing mice (control) or treated with: Dox/Cyclo, ICRP, or Dox/Cyclo + ICRP. Hematological parameters were analyzed with the hematology analyzer Sysmex XS 1000. Values are presented as mean ± SD ($p \leq 0.05$) ($n = 5$). Statistical significance was determined by the Tukey post hoc test. There is no statistical difference between data labeled with the same letter ([a,b,c]).

Table 2
Biochemical parameters of tumor-bearing mice.

	Control	Dox/Cyclo	ICRP	Dox/Cyclo + ICRP	Normal range
Total bilirubin (mg/dL)	0.07 ± 0.01	0.07 ± 0.01	0.085 ± 0.01	0.06 ± 0.02	0.00–1.40
Direct bilirubin (mg/dL)	0.03 ± 0.01	0.04 ± 0.01	0.055 ± 0.01	0.02 ± 0.02	0.00–0.50
Indirect bilirubin (mg/dL)	0.04 ± 0.01	0.03 ± 0.00	0.03 ± 0.01	0.04 ± 0.04	0.00–0.90
Total protein (g/dL)	5.15 0.07	5.25 ± 0.21	5.05 ± 0.07	5.10 ± 0.14	6.0–8.1
Albumin (g/dL)	3.6 ± 0.01	3.65 ± 0.07	3.65 ± 0.01	3.65 ± 0.21	3.0–5.2
Globulin (g/dL)	1.55 ± 0.07	1.6 ± 0.28	1.4 ± 0.01	1.45 ± 0.07	1.5–3.3
Aspartate aminotransferase (UI/L)	276.5 ± 20[a]	97 ± 1.41[b]	152 ± 59.4[c]	98 ± 2.83[b]	4–37
Alanine aminotransferase (U/L)	187 ± 25[a]	59.5 ± 0.71[b]	90.5 ± 40.31[c]	56 ± 8.49[b]	4–41
Alkaline phosphatase (U/L)	124 ± 19.8	103 ± 5	99 ± 11.31	88 ± 14.84	40–129

After 4T1 cell inoculation (day 30), peripheral blood was collected from untreated 4T1 tumor-bearing mice (control) or treated with: Dox/Cyclo, ICRP, or Dox/Cyclo + ICRP. Biochemical parameters were analyzed with the chemistry analyzer COBAS INTEGRA® 400 plus. Values are presented as mean ± SD ($p \leq 0.05$) ($n = 5$). Statistical significance was determined by the Tukey post hoc test. There is no statistical difference between data labeled with the same letter ([a,b,c]).

affected in a treatment-dependent manner. In our study, it is interesting to note that the use of ICRP or Dox/Cyclo as monotherapies correlate with the tumor reduction and decrease of IL-6 in the TME. However, a better response was obtained by the combined treatment of Dox/Cyclo + ICRP, resulting in an increase of pro-inflammatory cytokines.

The combination treatment increased $CD8^+$ and memory T cells both at systemic and TME levels. $CD8^+$ T cells are associated with immune surveillance and good patient prognosis [8]. $CD8^+$ T cells maintained their effector phenotype, evidenced by tumor reduction, production of TNF-α and IFN-γ, and increase of memory T cells, suggesting that the treatment with ICRP alone or combined elicited an anti-tumor immune response.

The Dox/Cyclo treatment increased MDSC within the TME (correlating with increased IDO levels) and peripheral blood T reg cells. It is worth mentioning that, although low-dose cyclophosphamide is used to decrease T reg cells, we administered the therapeutic dose [32]; the therapeutic dose of cyclophosphamide and doxorubicin increases MDSC in cancer patients [33]. T reg and MDSC induce local and systemic immune tolerance *via* IDO production, impairing antigen presentation and therefore enabling the immune escape and metastasis of breast cancer cells [34].

Our findings indicate that Dox/Cyclo + ICRP therapy administration elicited a strong immune response against breast cancer cells. To corroborate this, we performed the splenocyte/4T1 cells co-culture. We observed a higher cytotoxic response with splenocytes from the control group, indicating the capacity of peripheral immunity to recognize and eliminate 4T1, however not at TME level, as observed by tumor progression. Splenocytes from Dox/Cyclo group did not eliminated 4T1 cancer cells, suggesting an impaired cytotoxic activity at systemic level. Myelosuppression is strongly associated with Dox/Cyclo regimens and drug-induced myelosuppression impairs tumor immunity [35]. On the other hand, the cytotoxic activity of splenocytes was partially recovered by the combination of Dox/Cyclo with ICRP.

The putative mechanism of action by which ICRP increases Dox/Cyclo anti-tumor effect is outlined below. The combination of Dox/Cyclo + ICRP induced cancer cell mitosis arrest and death, as evidenced by Ki-67 decrease and cleaved caspase 3 increase [36]. In the TME cancer cells produce various immunosuppressive molecules, including IL-10, PD-L1 and Gal-3 [37]. Cancer cell cytoreduction in addition to the immunomodulatory properties of ICRP [38] allowed the remodeling of non-cancer elements within the tumor toward an increase of $CD8^+$ and memory T cells phenotype and a decrease of T reg cells and CAFs associated factors VEGF and α-SMA [20].

Coupled with this process there was a release of TNF-α, IFN-γ and IL-6 that correlate with the recruitment of T cells, macrophages, and dendritic cells [39,40,41,42,43]. These cells orchestrate the induction and effector phase of tumor-specific immunity, as demonstrated with the co-culture of splenocytes with 4T1 cells that resulted in cancer-specific cell death.

We suggest that further experiments with immunodeficient mice (T, B, natural killer, and macrophages) should be performed to clarify the role of ICRP as a modifier of the immune response at systemic and intratumoral levels. We would also like to mention, that despite all treatments decreased tumor volume and increased mice survival, it would be of interest to evaluate the efficacy of achieving tumor regression in other breast cancer models.

Finally, we evaluated major organs (brain, lungs, heart, liver, and spleen) and no histopathological changes were observed in treated mice. It is worth mentioning that a major concern with combined therapies for cancer is the adverse side effects.

Hematological and biochemical parameters are also important diagnostic tools for disease monitoring and patient wellbeing [44]. There was a mild leukocytosis in the control group and elevated levels of aspartate aminotransferase and alanine aminotransferase in all groups, with the control group being the highest. However, no damage was observed in the liver histological analysis, therefore the mild leukocytosis and elevated enzymes seem to indicate a chronic inflammation process (tumor itself), that did not affect performance and life quality of treated mice. These results show that our combined treatment has good biocompatibility.

In conclusion, we suggest that ICRP modifies the TME and immune response potentiating or prolonging the anti-tumor activity of Dox/Cyclo chemotherapy in a TNBC murine model. Furthermore, ICRP can serve as a basis for therapies that target multiple components of the TME and immune response against cancer cells.

5. Statement of ethics approval

All animal procedures were performed according to the official Mexican norm of animal welfare NOM-033-SAG/ZOO-2014 and approved by the Comité de Ética Interno de Bienestar Animal (CEIBA) de la Facultad de Ciencias Biológicas de la Universidad Autónoma de Nuevo León.

6. Consent for publication

Not applicable

Funding

This work was supported by the Laboratorio de Inmunología y Virología de la Universidad Nacional Autónoma de Nuevo León, México; by “Fondo Sectorial de Investigación para la Educación”, grant A1-S-35951, CONACYT, México; and by LONGEVEDEN S.A de C.V.

Authors’ contribution

SESK was involved in the experimental execution of the project, data interpretation and writing of the manuscript. MAFM devised the project and was involved in data interpretation and writing of the

manuscript. CRP provided overall supervision and guidance for the project. FTM established the immunohistochemistry protocol and helped analyze the data. The remaining authors provided valuable contributions to the final manuscript. All authors read and approved the final manuscript.

Availability of data and materials

The data sets used and analyzed during the current study are available from the corresponding author upon reasonable request.

Declaration of Competing Interest

The authors declare that they have no competing interests.

Acknowledgements

We thank Alejandra Elizabeth Arreola Triana for article revision; Universidad Autónoma de Nuevo León UANL, Facultad de Ciencias Biológicas, Laboratorio de Inmunología y Virología, P.O. Box 46 “F”, 66455 San Nicolás de los Garza, NL, México for funding and facilities provided; “Fondo Sectorial de Investigación para la Educación”, grant A1-S-35951, CONACYT, México; and LONGEVEDEN S.A de C.V for funding.

References

[1] F. Bray, J. Ferlay, I. Soerjomataram, R.L. Siegel, L.A. Torre, A. Jemal, Global cancer statistics 2018: GLOBOCAN estimates of incidence and mortality worldwide for 36 cancers in 185 countries, CA Cancer J. Clin. 68 (6) (2018) 394–424, https://doi.org/10.3322/caac.21492.

[2] M. Shoaib, S.A. Ahmed, Role of natural herbs and phytochemicals to minimize tumor and economic burden in breast cancer treatment, Breast Cancer Targets Ther. 8 (2016) 241–242, https://doi.org/10.2147/BCTT.S125826.

[3] P. Schmid, S. Adams, H.S. Rugo, A. Schneeweiss, C.H. Barrios, H. Iwata, et al., Atezolizumab and nab-paclitaxel in advanced triple-negative breast cancer, N. Engl. J. Med. 379 (22) (2018) 2108–2121, https://doi.org/10.1056/NEJMoa1809615.

[4] S.J. Isakoff, Triple-negative breast cancer: role of specific chemotherapy agents, Cancer J. 16 (1) (2010) 53–61, https://doi.org/10.1097/PPO.0b013e3181d24ff7.

[5] Y. Li, Y. Liang, Y. Sang, X. Song, H. Zhang, Y. Liu, et al., MiR-770 suppresses the chemo-resistance and metastasis of triple negative breast cancer via direct targeting of STMN1, Cell Death Dis. 9 (1) (2018) 1–12, https://doi.org/10.1038/s41419-017-0030-7.

[6] S. Paget, The distribution of secondary growths in cancer of the breast, Lancet 133 (3421) (1889) 571–573, https://doi.org/10.1016/S0140-6736(00)49915-0.

[7] M. Binnewies, E.W. Roberts, K. Kersten, V. Chan, D.F. Fearon, M. Merad, et al., Understanding the tumor immune microenvironment (TIME) for effective therapy, Nat. Med. 24 (5) (2018) 541–550, https://doi.org/10.1038/s41591-018-0014-x.

[8] C. Roma-Rodrigues, R. Mendes, P. Baptista, A. Fernandes, Targeting tumor microenvironment for cancer therapy, Int. J. Mol. Sci. 20 (4) (2019) 1–31, https://doi.org/10.3390/ijms20040840.

[9] E.E. Coronado-Cerda, M.A. Franco-Molina, E. Mendoza-Gamboa, H. Prado-García, L.G. Rivera-Morales, P. Zapata-Benavides, et al., “*In vivo*” chemoprotective activity of bovine dialyzable leukocyte extract in mouse bone marrow cells against damage induced by 5-fluorouracil, J. Immunol. Res. 2016 (2016) 1–10, https://doi.org/10.1155/2016/6942321.

[10] M.A. Franco-Molina, E. Mendoza-Gamboa, L. Castillo-León, R.S. Tamez-Guerra, C. Rodríguez-Padilla. Bovine dialyzable leukocyte extract modulates the nitric oxide and pro-inflammatory cytokine production in lipopolysaccharide-stimulated murine peritoneal macrophages *in vitro*, J. Med. Food 8 (1) (2005) 20–26, https://doi.org/10.1089/jmf.2005.8.20.

[11] M.A. Franco-Molina, E. Mendoza-Gamboa, D. Miranda-Hernández, P. Zapata-Benavides, L. Castillo-León, C. Isaza-Brando, et al., *In vitro* effects of bovine dialyzable leukocyte extract (bDLE) in cancer cells, Cytotherapy. 8 (4) (2006) 408–414, https://doi.org/10.1080/14653240600847266.

[12] M. Rodríguez-Salazar, M.A. Franco-Molina, E. Mendoza-Gamboa, A. Martínez-Torres, P. Zapata-Benavides, J. López-González, et al., The novel immunomodulator IMMUNEPOTENT CRP combined with chemotherapy agent increased the rate of immunogenic cell death and prevented melanoma growth, Oncol. Lett. 14 (1) (2017) 844–852, https://doi.org/10.3892/ol.2017.6202.

[13] M.A. Franco-Molina, S.E. Santana-Krímskaya, E.E. Coronado-Cerda, C.E. Hernández-Luna, D.G. Zarate-Triviño, P. Zapata-Benavides, et al., Increase of the antitumour efficacy of the biocompound IMMUNEPOTENT CRP by enzymatic treatment, Biotechnol. Biotechnol. Equip. 32 (2018) 1028–1035, https://doi.org/10.1080/13102818.2018.1460622.

[14] M.A. Franco-Molina, S.E. Santana-Krímskaya, C. Rodríguez-Padilla, Air pouch model: an alternative method for cancer drug discovery, in: R. Ali Mehanna (Ed.), Cell Culture, IntechOpen, 2019, , https://doi.org/10.5772/intechopen.79503.

[15] A. Faustino-Rocha, P.A. Oliveira, J. Pinho-Oliveira, C. Teixeira-Guedes, R. Soares-Maia, R.G. da Costa, et al., Estimation of rat mammary tumor volume using caliper and ultrasonography measurements, Lab Anim. (NY) 42 (2013) 217–224, https://doi.org/10.1038/laban.254.

[16] F. Patera, A. Cudzich-Madry, Z. Huang, M. Fragiadaki, Renal expression of JAK2 is high in polycystic kidney disease and its inhibition reduces cystogenesis, Sci. Rep. 9 (2019) 1–10, https://doi.org/10.1038/s41598-019-41106-3.

[17] Q. Luo, L. Zhang, C. Luo, M. Jiang, Emerging strategies in cancer therapy combining chemotherapy with immunotherapy, Cancer Lett. 454 (2019) 191–203, https://doi.org/10.1016/j.canlet.2019.04.017.

[18] X. Liu, S. Jiang, X. Tian, Y. Jiang, Expression of cleaved caspase-3 predicts good chemotherapy response but poor survival for patients with advanced primary triple-negative breast cancer, Int. J. Clin. Exp. Pathol. 11 (9) (2018) 4363–4373.

[19] X. Tian, Y. Li, Y. Shen, Q. Li, Q. Wang, L. Feng, Apoptosis and inhibition of proliferation of cancer cells induced by cordycepin, Oncol. Lett. 10 (2) (2015) 595–599.

[20] F. Wang, W. Sun, J. Zhang, Y. Fan, Cancer-associated fibroblast regulation of tumor neo-angiogenesis as a therapeutic target in cancer (Review), Oncol. Lett. 17 (2019) 3055–3065, https://doi.org/10.3892/ol.2019.9973.

[21] E. Bridges, A.L. Harris, Vascular-promoting therapy reduced tumor growth and progression by improving chemotherapy efficacy, Cancer Cell 27 (2015) 7–9, https://doi.org/10.1016/j.ccell.2014.12.009.

[22] K. Murata, T. Tsukahara, T. Torigoe, Cancer immunotherapy and immunological memory, Jpn J Clin Immunol. 39 (2016) 18–22, https://doi.org/10.2177/jsci.39.18.

[23] F.J. Esteva, V.M. Hubbard-Lucey, J. Tang, L. Pusztai, Immunotherapy and targeted therapy combinations in metastatic breast cancer, Lancet Oncol. 20 (2019) e175–e186, https://doi.org/10.1016/S1470-2045(19)30026-9.

[24] Y.I. Jeong, S.W. Kim, I.D. Jung, J.S. Lee, J.H. Chang, C.M. Lee, et al., Curcumin suppresses the induction of indoleamine 2,3-dioxygenase by blocking the janus-activated kinase-protein kinase cδ-STAT1 signaling pathway in interferon-γ-stimulated murine dendritic cells, J. Biol. Chem. 284 (2009) 3700–3708, https://doi.org/10.1074/jbc.M807328200.

[25] L. Xu, Y. Zhang, K. Tian, X. Chen, R. Zhang, X. Mu, et al., Apigenin suppresses PD-L1 expression in melanoma and host dendritic cells to elicit synergistic therapeutic effects, J. Exp. Clin. Cancer Res. 37 (2018) 261, https://doi.org/10.1186/s13046-018-0929-6.

[26] E.I. Buchbinder, A. Desai, CTLA-4 and PD-1 pathways: similarities, differences, and implications of their inhibition, Am. J. Clin. Oncol. 39 (2016) 98–106, https://doi.org/10.1097/COC.0000000000000239.

[27] Z. Li, Y. Qiu, W. Lu, Y. Jiang, J. Wang, Immunotherapeutic interventions of triple negative breast cancer, J. Transl. Med. 16 (2018) 147, https://doi.org/10.1186/s12967-018-1514-7.

[28] T. Gruosso, M. Gigoux, V.S.K. Manem, N. Bertos, D. Zuo, I. Perlitch, et al., Spatially distinct tumor immune microenvironments stratify triple-negative breast cancers, J. Clin. Invest. 129 (2019), https://doi:1785-800.10.1172/JCI96313.

[29] S.Y. Hwang, S. Park, Y. Kwon, Recent therapeutic trends and promising targets in triple negative breast cancer, Pharmacol. Ther. 199 (2019) 30–57, https://doi.org/10.1016/j.pharmthera.2019.02.006.

[30] M.J.V. White, D. Roife, R.H. Gomer, Galectin-3 binding protein secreted by breast cancer cells inhibits monocyte-derived fibrocyte differentiation, J. Immunol. 195 (2015) 1858–1867, https://doi.org/10.4049/jimmunol.1500365.

[31] N. Ahmad, A. Ammar, S.J. Storr, A.R. Green, E. Rakha, I.O. Ellis, et al., IL-6 and IL-10 are associated with good prognosis in early stage invasive breast cancer patients, Cancer Immunol. Immunother. 67 (2018) 537–549, https://doi.org/10.1007/s00262-017-2106-8.

[32] R. Abu Eid, G.S.E. Razavi, M. Mkrtichyan, J. Janik, S.N. Khleif, Old-school chemotherapy in immunotherapeutic combination in cancer, a low-cost drug repurposed, Cancer Immunol. Res. 4 (2016) 377–382, https://doi.org/10.1158/2326-6066.CIR-16-0048.

[33] C.M. Diaz-Montero, M.L. Salem, M.I. Nishimura, E. Garrett-Mayer, D.J. Cole, A.J. Montero, Increased circulating myeloid-derived suppressor cells correlate with clinical cancer stage, metastatic tumor burden, and doxorubicin–cyclophosphamide chemotherapy, Cancer Immunol. Immunother. 58 (2009) 49–59, https://doi.org/10.1007/s00262-008-0523-4.

[34] F. Li, Y. Zhao, L. Wei, S. Li, J. Liu, Tumor-infiltrating Treg, MDSC, and IDO expression associated with outcomes of neoadjuvant chemotherapy of breast cancer, Cancer Biol. Ther. 19 (2018) 695–705, https://doi.org/10.1080/15384047.2018.1450116.

[35] K. Tecza, J. Pamula-Pilat, J. Lanuszewska, D. Butkiewicz, E. Grzybowska, Pharmacogenetics of toxicity of 5-fluorouracil, doxorubicin and cyclophosphamide chemotherapy in breast cancer patients, Oncotarget 9 (2018) 9114–9136, https://doi.org/10.18632/oncotarget.24148.

[36] A.S. Nahed, M.Y. Shaimaa, Ki-67 as a prognostic marker according to breast cancer molecular subtype, Cancer Biol. Med. 13 (4) (2016) 496–594, https://doi.org/10.20892/j.issn.2095-3941.2016.0066.

[37] H. Nishio, T. Yaguchi, J. Sugiyama, H. Sumimoto, K. Umezawa, T. Iwata, et al., Immunosuppression through constitutively activated NF-κB signalling in human ovarian cancer and its reversal by an NF-κB inhibitor, Br. J. Cancer 110 (12) (2014) 2965–2974, https://doi.org/10.1038/bjc.2014.251.

[38] M.A. Franco Molina, S.E. Santana-Krímskaya, R. Támez-Guerra, C. Rodríguez-Padilla, A review of IMMUNEPOTENT CRP, a modifier of biological response: efficacy and current practice, Biomed J Sci Tech Res. 14 (1) (2019) 10477–10480 https://doi:10.26717.BJSTR.2019.14.002509.

[39] T. Calzascia, M. Pellegrini, H. Hall, L. Sabbagh, N. Ono, A.R. Elford, et al., TNF-α is

critical for antitumor but not antiviral T cell immunity in mice, J. Clin. Invest. 117 (12) (2007) 3833–3845, https://doi.org/10.1172/JCI32567.
[40] G. Arango Duque, A. Descoteaux, Macrophage cytokines: involvement in immunity and infectious diseases, Front. Immunol. 5 (2014) 1–12, https://doi.org/10.3389/fimmu.2014.00491.
[41] L. Frasca, M. Nasso, F. Spensieri, G. Fedele, R. Palazzo, F. Malavasi, et al., IFN-γ arms human dendritic cells to perform multiple effector functions, J. Immunol. 180 (3) (2008) 1471–1481, https://doi.org/10.4049/jimmunol.180.3.1471.
[42] S. Hervas-Stubbs, J.L. Perez-Gracia, A. Rouzaut, M.F. Sanmamed, A. Le Bon, I. Melero, Direct effects of type I interferons on cells of the immune system, Clin. Cancer Res. 17 (9) (2011) 2619–2627, https://doi.org/10.1158/1078-0432.CCR-10-1114.
[43] D.T. Fisher, M.M. Appenheimer, S.S. Evans, The two faces of IL-6 in the tumor microenvironment, Semin. Immunol. 26 (1) (2014) 38–47, https://doi.org/10.1016/j.smim.2014.01.008.
[44] V.S. Swapna, V. Sudhakar, D. Javerappa, Study of liver function tests in breast carcinoma patients before and after chemotherapy, Int J Biotechnol Biochem. 14 (3) (2018) 177–184.